



## Photoacoustic characterization of a twolayer system

A. M. Mansanares, H. Vargas, F. Galembeck, J. Buijs, and D. Bicanic

Citation: *J. Appl. Phys.* **70**, 7046 (1991); doi: 10.1063/1.349782

View online: <http://dx.doi.org/10.1063/1.349782>

View Table of Contents: <http://jap.aip.org/resource/1/JAPIAU/v70/i11>

Published by the [American Institute of Physics](#).

---

### Related Articles

A model for the effective thermal conductivity of metal-nonmetal particulate composites  
*J. Appl. Phys.* **111**, 044319 (2012)

Thermoelectric efficiency of topological insulators in a magnetic field  
*J. Appl. Phys.* **111**, 07E319 (2012)

Effective medium formulation for phonon transport analysis of nanograined polycrystals  
*J. Appl. Phys.* **111**, 014307 (2012)

On the accuracy of classical and long wavelength approximations for phonon transport in graphene  
*J. Appl. Phys.* **110**, 113510 (2011)

A study of the impact of dislocations on the thermoelectric properties of quantum wells in the Si/SiGe materials system  
*J. Appl. Phys.* **110**, 114508 (2011)

---

### Additional information on *J. Appl. Phys.*


Journal Homepage: <http://jap.aip.org/>

Journal Information: [http://jap.aip.org/about/about\\_the\\_journal](http://jap.aip.org/about/about_the_journal)

Top downloads: [http://jap.aip.org/features/most\\_downloaded](http://jap.aip.org/features/most_downloaded)

Information for Authors: <http://jap.aip.org/authors>

## ADVERTISEMENT

	<b>Working @ low temperatures?</b> Contact Janis for Cryogenic Research Equipment <a href="http://www.janis.com">Click here</a> to browse our site at <b>www.janis.com</b>	
---	--	---

# Photoacoustic characterization of a two-layer system

A. M. Mansanares and H. Vargas

*Instituto de Física, Universidade Estadual de Campinas, 13.100-Campinas, SP, Brazil*

F. Galembeck

*Instituto de Química, Universidade Estadual de Campinas, 13.100-Campinas, SP, Brazil*

J. Buijs and D. Bicanic

*Department of Agricultural Engineering and Physics, Agricultural University, Duivendaal 1, 6701 AP Wageningen, The Netherlands*

(Received 15 April 1991; accepted for publication 28 June 1991)

In this paper the use of the so-called open photoacoustic cell for thermal characterization of two-layer systems of variable thickness is described. It is shown that the thermal diffusivity as well as the thermal conductivity are completely determined, based upon the effective sample model widely used in heat-transfer problems.

## I. INTRODUCTION

During the last decade, several methods have been developed to determine thermal diffusivities with high precision by means of photothermal effects. (For a review, see Ref. 1.) The most widely used method is based upon the photoacoustic (PA) effect. The PA effect looks directly at the heat generated in a sample (due to nonradiative de-excitation processes) following the absorption of modulated light. In the conventional experimental arrangement a sample is enclosed in an airtight cell and exposed to a chopped light beam. As a result of the periodic heating of the sample, the pressure in the chamber oscillates at the chopping frequency; this is detected by a sensitive microphone coupled to the cell. The resulting signal depends not only on the amount of heat generated in the sample (i.e., on the optical-absorption coefficient and the light-into-heat conversion efficiency of the sample) but also on how the heat diffuses through the sample, that is, on the thermal diffusivity  $\alpha$ . Apart from its own intrinsic importance, its determination provides the value of the thermal conductivity  $k$ , when the density  $\rho$  and the specific heat  $c$  at constant pressure are known, since

$$\alpha = k/\rho c. \quad (1)$$

Thermal diffusivities of several materials can be accurately measured by the PA technique and various setups have been developed.<sup>2,3</sup> Recently, an improved gas microphone detection called the open photoacoustic cell (OPC) technique, especially suited for measuring thermal diffusivities, has been proposed.<sup>4</sup> The method may either be used as a spectroscopic technique to monitor chemical and structural changes<sup>5</sup> or for monitoring thermal properties.<sup>6,7</sup>

In a recent paper<sup>8</sup> we described a study of a series two-layer system, in which the sample thermal properties ( $\alpha$  and  $k$ ) were investigated using two different PA techniques. The usefulness of the effective thermal diffusivity model for the description of the thermal diffusivity of a two-layer system was demonstrated as a function of the constituent materials' thermal properties ( $\alpha_i$  and  $k_i$ ). The systems studied were plate-glass Mylar and aluminum coated with white paint.

In the present paper the OPC technique is used for the determination of the thermal diffusivity of a two-layer system consisting of high-density polyethylene (HDPE) and polyvinyl chloride (PVC). This is a model for coextrudate films. Coextrudates are materials of considerable technical importance currently, and we are interested in learning to what extent photoacoustic techniques may help in their characterization.

## II. EFFECTIVE THERMAL DIFFUSIVITY

Consider the two-layer system shown schematically in Fig. 1 consisting of a material 1 of thickness  $l_1$  and of a material 2 with thickness  $l_2$ , both having the same cross section. Let  $l = l_1 + l_2$  denote the total sample thickness,  $\alpha_i$  the thermal diffusivity,  $\rho_i$  the density,  $c_i$  the specific heat at constant pressure, and  $k_i$  the thermal conductivity of material  $i$  ( $i = 1, 2$ ). From the analogy between thermal and electrical resistances widely used in heat-transfer problems,<sup>9</sup> the effective thermal resistance  $r$  of this series two-layer system may be written as

$$r = l/k = r_1 + r_2, \quad (2)$$

where  $k$  is the effective thermal conductivity of the composite sample, and  $r_i = l_i/k_i$  is the thermal resistance of layer  $i$ . From Eq. (2),

$$k = lk_1k_2/(l_1k_2 + l_2k_1). \quad (3)$$

On the other hand, the effective heat capacity  $V\rho c$  of the composite sample is given by

$$V\rho c = V_1\rho_1c_1 + V_2\rho_2c_2. \quad (4)$$

Substituting Eqs. (3) and (4) into Eq. (1) and performing some straightforward algebra, we can write the thermal diffusivity of the two-layer system as

$$\alpha = \frac{1}{(x^2/\alpha_1) + (1-x)^2/\alpha_2 + x(1-x)(\lambda/\alpha_1 + 1/\lambda\alpha_2)}, \quad (5)$$

where  $x = l_1/l$  measures the thickness fraction of material 1 in the composite sample, and  $\lambda = k_1/k_2$ . Equation (5) implies that the thermal diffusivity of the composite sample

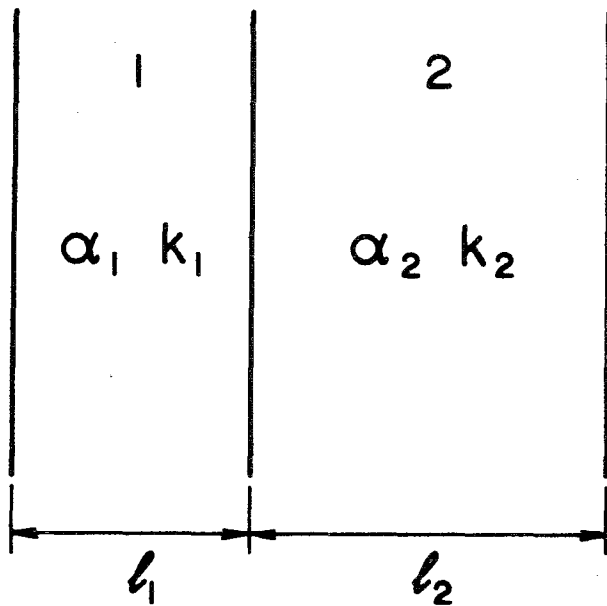


FIG. 1. Geometry for the two-layer system.

depends not only on the thermal diffusivity of its constituent materials but also on the ratio of their thermal conductivities.

### III. EXPERIMENT

The open photoacoustic cell detector is shown in Fig. 2(a). Basically, the radiation absorbing material is directly mounted to a commercial electret microphone. This type of photoacoustic detector requires neither an additional transducing medium, such as, for example, the confined layer of air encountered with the conventional PA cell, nor the time-consuming machining of the cell. The typical design of an electret microphone consists of a metalized electret diaphragm (12  $\mu\text{m}$  Teflon with a 500–1000- $\text{\AA}$ -thick deposited metal electrode) and a metal back plate separated from the diaphragm by an air gap (45  $\mu\text{m}$ ). The metal layer and the back plate are connected through a resistor  $R$ . The front sound inlet is a circular hole of 2 mm diam, and the front air chamber adjacent to the metalized face of the diaphragm is approximately 1 mm long. As a result of the periodic heating of the sample by the absorption of modulated light, the pressure in the front chamber oscillates at the chopping frequency, causing diaphragm deflections, which generate a voltage  $V$  across the resistor  $R$ . This voltage  $V$  is subsequently fed into a field-effect-transistor (FET) preamplifier already built into the microphone capsules. The FET polarization voltage is usually between 1.5 and 3.0 V. The experimental setup for the measurement of thermal diffusivities consists of a 160-W tungsten lamp, the polychromatic beam of which is mechanically chopped and focused onto the sample. The signal from the microphone is connected to a lock-in amplifier (PAR Model 124) through which both the signal amplitude and the phase are stored, as a function of the modulation frequency, in a microcomputer.

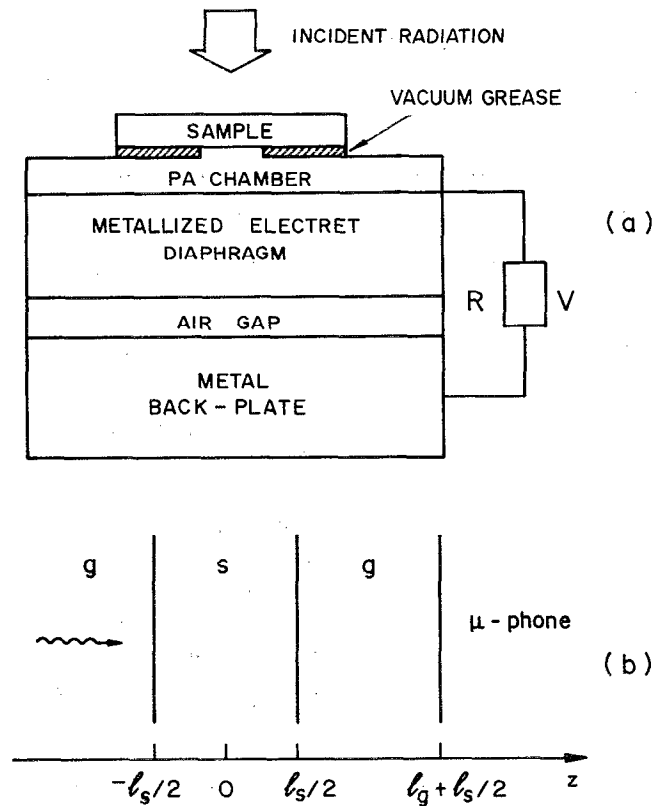


FIG. 2. (a) Cross section of the open photoacoustic cell detector and (b) geometry of the open photoacoustic cell.

### IV. METHODOLOGY

To understand the PA signal monitoring of a sample using the open photoacoustic cell detector, we should examine the modulation frequency dependence of the detected signal. The usual way for extracting information about the thermal diffusivity of the sample is to analyze the data when recording the magnitude and phase of the PA signal versus the modulation frequency.

According to the one-dimensional model of Rosencwaig and Gersho,<sup>10</sup> for the arrangement schematically shown in Fig. 2(b) the pressure fluctuation in the air chamber is given<sup>4</sup> by

$$P_{\text{th}} = \frac{\gamma P_0 I_0 (\alpha_g \alpha_s)^{1/2}}{2\pi l_g T_0 k_s f \sinh(l_s \sigma_s)} e^{j(\omega t - \pi/2)}, \quad (6)$$

where  $\gamma$  is the air specific-heat ratio,  $P_0(T_0)$  is the ambient pressure (temperature),  $I_0$  is the radiation intensity,  $f$  is the modulation frequency, and  $l_i$ ,  $k_i$ , and  $\alpha_i$  are the length, thermal conductivity, and thermal diffusivity of medium  $i$ , respectively. Here, the subscript  $i$  refers to the sample  $s$  and gas  $g$  media, and  $\sigma_i = (1 + j)a_i$ ,  $a_i = (\pi f / \alpha_i)^{1/2}$ , is the complex thermal-diffusion coefficient of medium  $i$ . In arriving at Eq. (6) it was assumed that the sample is optically opaque and that the heat flux into the surrounding air is negligible. For a thermally thin sample (i.e.,  $l_s \sigma_s \ll 1$ ), Eq. (6) reduces to

$$P_{th} \approx \frac{\gamma P_0 I_0 \alpha_s^{1/2} \alpha_s}{(2\pi)^{3/2} T_0 l_g k_s} \frac{e^{j(\omega t - 3\pi/4)}}{f^{3/2}} \quad (7)$$

In other words, the PA signal amplitude decreases as  $f^{-1.5}$  with increasing modulation frequency. On the contrary, for high modulation frequencies, when the sample is thermally thick (i.e.,  $l_s \alpha_s \gg 1$ ), one obtains

$$P_{th} \approx \frac{\gamma P_0 I_0 (\alpha_s \alpha_s)^{1/2} \exp[-l_s(\pi f/\alpha_s)^{1/2}]}{\pi T_0 l_g k_s f} \times e^{j(\omega t - \pi/2 - l_s \alpha_s)} \quad (8)$$

Equation (8) implies that, for a thermally thick sample, the amplitude of the PA signal decreases exponentially with the modulation frequency according to  $(1/f) \exp(-b\sqrt{f})$ , with  $b = l_s(\pi/\alpha_s)^{1/2}$ , while its phase  $\varphi$  decreases linearly with  $b\sqrt{f}$ . The thermal diffusivity  $\alpha_s$  can then be obtained from the high-modulation-frequency behavior of either the signal amplitude or its phase. As far as the signal amplitude is concerned,  $\alpha_s$  is obtained from the fitting coefficient  $b$  appearing as the argument of the exponent  $(-b\sqrt{f})$ . When using the signal-phase data,  $\alpha_s$  is obtained from the slope of the phase (as a function of  $\sqrt{f}$ ). However, in the case of plate-shaped solid samples, the contribution to the photoacoustic signal from the thermoelastic bending of the sample cannot be neglected, especially in the case of thermally thick samples, as has been demonstrated by Charpentier, Lepoutre, and Bertrand<sup>11</sup> and Leite *et al.*<sup>12</sup> This effect is essentially due to the temperature gradient set within the sample along the thickness direction. The existence of the expansion of the sample parallel to its surface induces thereby a bending along the thickness direction (i.e., the vibrating sample acts as a mechanical piston-drum effect). In the thermally thick regime, the pressure fluctuation in the air chamber of the open photoacoustic cell detector resulting from the thermoelastic displacement, for an optically opaque sample, is given<sup>11,12</sup> by

$$P_{el} \approx \frac{3\alpha_T R^4 \gamma P_0 I_0 \alpha_s}{4\pi R_c^2 l_g k_s f} \left[ \left(1 - \frac{1}{z}\right)^2 + \frac{1}{z^2} \right]^{1/2} e^{j(\omega t + \pi/2 + \varphi)} \quad (9)$$

where  $z = b\sqrt{f}$ ,  $\varphi = \tan^{-1}[1/(z-1)]$ , and  $\alpha_T$  is the sample thermal-expansion coefficient,  $R$  the radius of the front hole of the microphone, and  $R_c$  the radius of the front air chamber. Equation (9) means that the thermoelastic contribution, at high-modulation frequencies (such that  $z \gg 1$ ) varies as  $f^{-1}$ , and its phase  $\varphi_{el}$  follows the expression

$$\varphi_{el} \approx \varphi_0 + \tan^{-1}[1/(z-1)] \quad (10)$$

Thus, for a thermally thick sample, if the thermoelastic contribution is dominant, the thermal diffusivity can be evaluated from the modulation-frequency dependence of the signal phase [Eq. (10)].

## V. RESULTS AND DISCUSSION

The samples used were two-layer disk-shaped (8 mm diam) films of HDPE (layer 1), 35 and 50  $\mu\text{m}$  thick, and PVC (layer 2), 22 and 80  $\mu\text{m}$  thick. The disks were held

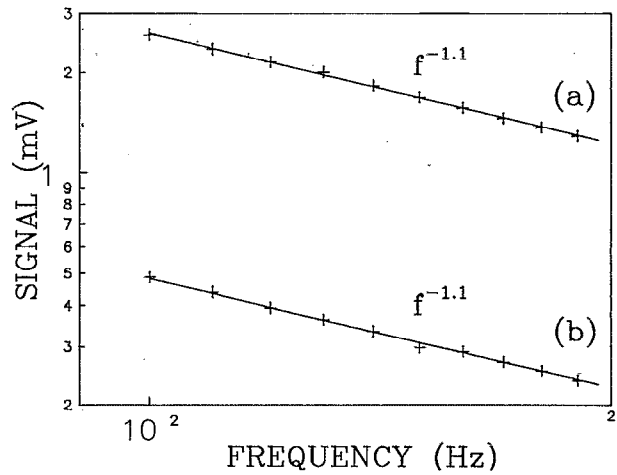


FIG. 3. The dependence of the PA signal on the modulation frequency for (a) the 22- $\mu\text{m}$ -thick PVC foil and (b) the HDPE(50  $\mu\text{m}$ )-PVC(22  $\mu\text{m}$ ) composite sample.

together by capillarity using an extremely thin layer of diffusion pump silicone oil. The implicit condition for optical opaqueness [meaning that all the incident radiation is fully absorbed at the surface  $z = -l_s/2$ , see Fig. 2(b)]; required in arriving at Eqs. (6) and (9), was met by using a circular Al foil (20  $\mu\text{m}$  thick and 3 mm in diameter), attached to the front side of the sample, also using a thin layer of oil. This Al foil is thermally thin for modulation frequencies up to some few kHz ( $\alpha_{Al} = 0.92 \text{ cm}^2/\text{s}$ ), so that it introduces neither significant attenuation in the PA signal amplitude nor significant delay in its phase. The samples were placed to cover the top opening of the microphone and affixed by means of vacuum grease [Fig. 2(a)]. All the experiments were carried out in the 100–200-Hz modulation-frequency range. In this frequency range the microphone response is flat,<sup>13</sup> and using the typical values for the HDPE and PVC thermal diffusivities,<sup>4,12</sup> it is assured that the four polymer foils above are thermally thick.

The thermal diffusivity of each constituent of this two-layer system was measured separately. In Fig. 3(a) the dependence of the PA signal amplitude on the modulation frequency for the 22- $\mu\text{m}$ -thick PVC foil is shown. This amplitude decays as  $f^{-1.1}$  instead of exhibiting the exponential behavior [see Eq. (8)] predicted by the thermal-diffusion model. The observed frequency dependence of the PA signal thus suggests [see Eq. (9)] that in this frequency range thermoelastic bending is the dominant mechanism responsible for the acoustic signal. In this case the thermal diffusivity is obtained from the fit of the phase in Eq. (10). Assuming  $\varphi_0$  and  $b$  as adjustable parameters, the thermal diffusivity is readily given by  $\alpha = \pi(l_s/b)^2$ . In Fig. 4(a) the signal phase is shown as a function of the modulation frequency for the 22- $\mu\text{m}$ -thick PVC sample. The solid curve represents the fit to the experimental-phase data by the theoretical expression given by Eq. (10), and the value found for the thermal diffusivity was  $\alpha = 0.7 \times 10^{-3} \text{ cm}^2/\text{s}$ . The same procedure was applied to the 35- $\mu\text{m}$ -thick

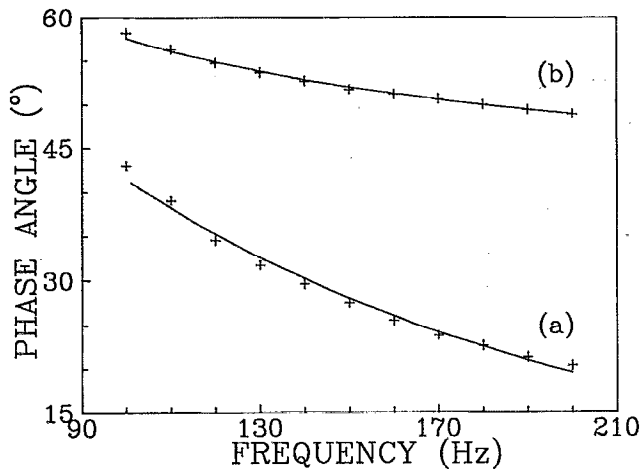


FIG. 4. PA signal phase angle dependence on the chopping frequency for (a) the 22- $\mu\text{m}$ -thick PVC foil and (b) the HDPE(50  $\mu\text{m}$ )-PVC(22  $\mu\text{m}$ ) composite sample. The solid curves represent the fit to the experimental data by Eq. (10).

HDPE foil and in this case we found  $\alpha = 3.0 \times 10^{-3} \text{ cm}^2/\text{s}$ . These values agree very well with those reported in the literature.<sup>4,12</sup>

After the determination of the separated constituents' thermal diffusivities, three two-layer samples were measured: HDPE(35  $\mu\text{m}$ )-PVC(22  $\mu\text{m}$ ), HDPE(50  $\mu\text{m}$ )-PVC(22  $\mu\text{m}$ ), and HDPE(35  $\mu\text{m}$ )-PVC(80  $\mu\text{m}$ ). Figure 3(b) gives the PA signal amplitude dependence on the modulation frequency for the HDPE(50  $\mu\text{m}$ )-PVC(22  $\mu\text{m}$ ) composite sample. The  $f^{-1.1}$  behavior indicates again that the main mechanism responsible for the acoustic signal is the thermoelastic bending. Figure 4(b) shows the PA signal phase dependence on the modulation frequency for this sample. The solid curve represents the fit to the experimental data by Eq. (10). Table I summarizes the values of the thermal diffusivity for the five samples studied.

Figure 5 gives the measured data for  $\alpha$  as a function of the thickness ratio  $x$  [ $x = l_1/(l_1 + l_2)$ , where the subscript 1 refers to the HDPE constituent]. The solid line represents the result of the fit of these data by Eq. (5), leaving  $\alpha_1, \alpha_2$  and  $\lambda = k_1/k_2$  as adjustable parameters. The data fit procedure yielded the following values for the adjustable parameters:  $\alpha_1 = 3.0 \times 10^{-3} \text{ cm}^2/\text{s}$ ,  $\alpha_2 = 0.7 \times 10^{-3} \text{ cm}^2/\text{s}$ , and  $\lambda = 2.0$ . The error in the data fit was 3% and the

TABLE I. Values of the HDPE-PVC system components' thickness, the ratio  $x$  of the HDPE thickness to the total system thickness, and the measured values of the thermal diffusivity, as obtained by the OPC technique.

$l_1$ ( $\mu\text{m}$ )	$l_2$ ( $\mu\text{m}$ )	$x$	$\alpha$ ( $\times 10^{-3} \text{ cm}^2/\text{s}$ )
0	22	0.00	0.7
35	80	0.30	1.0
35	22	0.61	1.6
50	22	0.69	1.6
35	0	1.00	3.0

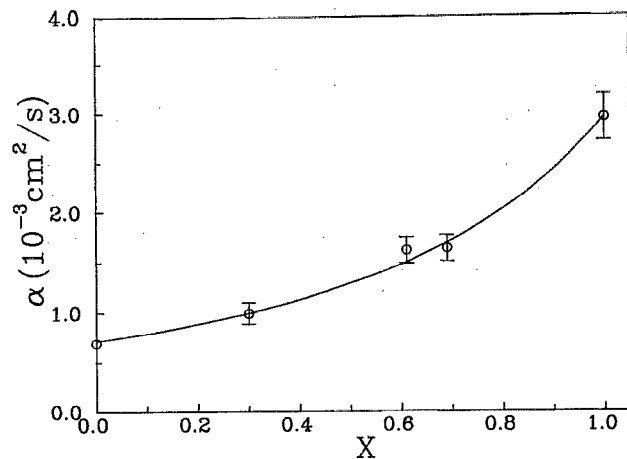


FIG. 5. Effective thermal-diffusivity data as obtained by the OPC technique for the HDPE-PVC samples as a function of  $x$ . The solid curve represents the fit to the data by Eq. (5).

values of  $\alpha_1$  and  $\alpha_2$  obtained from the fit are in accordance with the measured one. The value found for  $\lambda$  also agrees with the reported data for the thermal conductivities of HDPE and PVC in literature<sup>14</sup> ( $k_{\text{HDPE}} = 2.2\text{--}3.9 \text{ mW/cm K}$  and  $k_{\text{PVC}} = 1.4\text{--}1.6 \text{ mW/cm K}$ , at room temperature).

In conclusion, the usefulness of the effective thermal-diffusivity model for describing the thermal diffusivity of a two-layer sample composed by different polymer foils is demonstrated. The importance of this model is that, since the thermal properties of the separated constituents ( $\alpha_i$  and  $k_i$ ) are known, Eq. (5) gives directly the thermal diffusivity of a composite sample obtained for any thickness combination of these constituents. Another application of this model is in the determination of the thermal diffusivity and conductivity of a composed sample. The method consists in using the OPC technique for a two-layer system in which one of the layers is a standard material, such as a thin polymer foil for which both  $\alpha$  and  $k$  are well known. The other layer consists of the test sample for which  $\alpha$  and  $k$  are to be determined. By varying the standard layer thickness we can make, for instance, three two-layer samples. Using the OPC technique we can then generate a set of data for  $\alpha$  as function of  $x = l_1/(l_1 + l_2)$  (i.e., the ratio of the test sample thickness to the total system thickness). This data is then best fit to Eq. (5) from which the values of the thermal diffusivities as well as of the ratio  $\lambda$  of the thermal conductivities of each component are obtained. From the value of  $\lambda$ , the thermal conductivity of the test sample is readily found.

## ACKNOWLEDGMENTS

The authors are grateful to FAPESP and CNPq (Brazil) for partial support of this work and to Forchheim 4P GmbH (Germany) for supplying the polymer foil samples. This work was partially developed at the Department of Physics and Meteorology of the Agricultural University, Wageningen, The Netherlands.

- <sup>1</sup>H. Vargas and L. C. M. Miranda, *Phys. Rep.* **161**, 43 (1988).
- <sup>2</sup>M. J. Adams and G. Kirkbrigh, *Analyst* **102**, 281 (1977).
- <sup>3</sup>O. Pessoa, C. L. Cesar, N. A. Patel, H. Vargas, C. C. Ghizoni, and L. C. M. Miranda, *J. Appl. Phys.* **59**, 1316 (1986).
- <sup>4</sup>L. F. Perondi and L. C. M. Miranda, *J. Appl. Phys.* **62**, 2955 (1987).
- <sup>5</sup>M. V. Marquezini, N. Cella, E. C. da Silva, D. B. Serra, C. A. Lima, and H. Vargas, *Analyst* **115**, 341 (1990).
- <sup>6</sup>A. P. Neto, H. Vargas, N. F. Leite, and L. C. M. Miranda, *Phys. Rev. B* **40**, 3924 (1989).
- <sup>7</sup>N. Cella, H. Vargas, E. Galembeck, F. Galembeck, and L. C. M. Miranda, *J. Polymer Sci. Part C* **27**, 313 (1989).
- <sup>8</sup>A. M. Mansanares, A. C. Bento, H. Vargas, N. F. Leite, and L. C. M. Miranda, *Phys. Rev. B* **42**, 4477 (1990).
- <sup>9</sup>W. Karplus and W. W. Soroka, *Analog Methods* (McGraw-Hill, New York, 1959).
- <sup>10</sup>A. Rosencwaig and A. Gersho, *J. Appl. Phys.* **47**, 64 (1975).
- <sup>11</sup>P. Charpentier, F. Lepoutre, and L. Bertrand, *J. Appl. Phys.* **53**, 608 (1982).
- <sup>12</sup>N. F. Leite, N. Cella, H. Vargas, and L. C. M. Miranda, *J. Appl. Phys.* **61**, 3025 (1987).
- <sup>13</sup>A. C. Bento, M. M. F. Aguiar, H. Vargas, M. D. Silva, I. N. Bandeira, and L. C. M. Miranda, *Appl. Phys. B* **48**, 269 (1989).
- <sup>14</sup>Y. S. Touloukian, R. W. Powell, C. Y. Ho, and M. C. Nicolaou, *Thermophysical Properties of Matter* (Plenum, New York, 1970), Vol. 2.